Characterization of spirolide producing *Alexandrium ostenfeldii* (Dinophyceae) from the western Arctic

Urban Tillmann[a*], Anke Kremp[b], Pia Tahvanainen[b], and Bernd Krock[a]

[a] Alfred Wegener Institute, Am Handelshafen 12, D-27570 Bremerhaven, Germany

[b] Finnish Environment Institute, Marine Research Centre, Erik Palménin aukio 1, Helsinki 00560, Finland

[*] Corresponding author, phone: +49 471 4831 1470, e-mail: urban.tillmann@awi.de

ABSTRACT

Toxin producing dinoflagellates of the genus *Alexandrium* Halim represent a risk to Arctic environments and economies. This study provides the first record and a characterization of *Alexandrium ostenfeldii* in the western Arctic. During a cruise along the coasts of western and southern Greenland 36 isolates of the species were established in August 2012. Plankton samples taken at 3 different stations from the upper water layer at water temperatures of approx. 4-7 °C, contained low amounts of *A. ostenfeldii*. Sequencing of SSU and ITS-LSU rDNA and subsequent phylogenetic analyses identified all Greenland strains as members of a NW Atlantic spirolide producing phylogenetic clade. Molecular results were confirmed by morphological features typical for this group (= Group 5 of a recent ITS-LSU phylogeny of *A. ostenfeldii*). The Greenland isolates did not contain either Paralytic Shellfish Poisoning toxins or gymnodimines, but produced several spirolides. Altogether 12 different analogues were detected, of which only SPX-1, C, 20-meG and H have been described earlier. The remaining 8 spirolides have not been identified so far. Some of them were found to dominate the toxin profiles of a number of isolates. Among the 36 investigated strains spirolide composition varied considerably, particularly isolates from western Greenland (Station 516) exhibited a high diversity of analogues, with different profiles in nearly all 22 isolates. All of the 34 tested Greenland strains showed considerable lytic capacity when exposed to *Rhodomonas salina*.

Key-words: *Alexandrium ostenfeldii*, Greenland, spirolides, lytic activity

1. INTRODUCTION

World-wide, the majority of the toxic bloom-forming harmful algal species belong to the dinoflagellate genus *Alexandrium.* Species of *Alexandrium* are often globally distributed, occurring in a variety of habitats and all geographic zones (Taylor et al., 1995; Lilly et al., 2007). Many *Alexandrium* species are able to produce potent toxins, such as paralytic shellfish toxins (PSTs), which affect the neuromuscular, sensory, digestive and cardiovascular systems of human and other vertebrates (Hallegraeff, 1993; Selina et al., 2006) and account for most of the harmful events caused by members of the genus (Anderson et al., 2012). These algal toxins represent a serious risk for the environment and human health (Hallegraeff, 1993).

One of the less studied toxic species of the genus is *Alexandrium ostenfeldii*. It has been widely observed in temperate waters of Europe (Balech and Tangen, 1985), North America (Cembella et al., 2000a), the Russian Arctic (Okolodkov and Dodge, 1996) and Eastern Siberian Seas (Konovalova, 1991). There are also records of the occurrence of *A. ostenfeldii* from the coast of Spain (Fraga and Sanchez, 1985), the Mediterranean (Balech, 1995), New Zealand (Mackenzie et al., 1996), Peru (Sánchez et al., 2004) and Japan (Nagai et al., 2010). However, for a long time, *A. ostenfeldii* has been considered mainly as a background species, occurring at low cell concentrations mixed with other bloom forming dinoflagellates (Balech and Tangen, 1985; Moestrup and Hansen, 1988; John et al., 2003). Only in the past decade it has gained increasing attention when dense blooms of this species (or its synonym *A. peruvianum*) were reported e.g. from South America (Sánchez et al., 2004), the Northern Baltic Sea (Kremp et al., 2009), along the Adriatic coast of Italy (Ciminiello et al., 2006), the estuaries of the US East coast (Tomas et al., 2012), and, most recently, the Netherlands (Burson et al., 2014). It is not clear whether the recent increase in

bloom events is due to anthropogenic spreading or changing environmental conditions favoring bloom formation. Most of the recent blooms occurred during summer in coastal areas and were associated with warm water periods (e.g. Hakanen et al., 2012). Experimental studies indicate that increased water temperature has a favorable effect on *A. ostenfeldii* bloom populations and it has been suggested that changing climate conditions promote bloom formation (Kremp et al., 2012). The species produces PSP toxins (Hansen et al., 1992), spirolides (Cembella et al., 2000a) and gymnodimines (Van Wagoner et al., 2011), and all compounds may even occur together in one strain (Tomas et al., 2012). Thus, an increase of *A. ostenfeldii* bloom events with several potent toxins involved may represent a new risk to the environment that is associated with climate change.

Most of the global *A. ostenfeldii* records are from cold-water environments and the species has long been considered to have an arctic-boreal distribution (Okolodkov, 2005). It was originally described from the north-east coast of Iceland (Paulsen, 1904), and has thereafter been reported mainly from high latitude waters of the North Atlantic (Cembella et al., 2000a; Brown et al., 2010), Scandinavia (Tangen, 1983; Moestrup and Hansen, 1988) as well as arctic and subarctic waters of northern Siberia and the Russian Far East (Konovalova, 1991; Okolodkov, 2005; Selina et al., 2006). In a recent study on *A. tamarense* in Greenland, the presence of of *A. ostenfeldii* in the western Arctic was briefly mentioned (Baggesen et al., 2012).

It has been predicted that anthropogenic climate change is causing dramatic changes the Arctic area, including increased temperature (Screen and Simmonds, 2012) and rapid decline of glaciers, ice cover (Comiso et al., 2008), ice thickness (Kwok and Rothrock, 2009), and resulting in ice-free summer conditions in future. These changes will have large effects on many marine species including primary producers (Wassmann et al., 2008). Though the responses of the Arctic marine ecosystems to climate change are not well known, temperature

increase has been considered one of the changes affecting the performance, abundance and distribution of arctic organisms most significantly (Alcaraz et al., 2014). Temperature increase and larger ice-free regions have, for example, been suggested to expand the distribution ranges of HAB-species into or within the Arctic sea-area (Hallegraeff, 2010) and cause severe problems to the sensitive Arctic environment due to toxin production, and their accumulation in higher trophic levels.

Since *A. ostenfeldii* is present in arctic and subarctic waters, it could be one of the first harmful dinoflagellate species to be favored by the increase of water temperature and the predicted cascading effects of climate change in the ecosystem (Walsh et al., 2011). Alternatively, populations from temperate coastal waters of the North Atlantic or Pacific area may expand their ranges and cause toxic blooms in the Arctic. Most of the recently reported *A. ostenfeldii* blooms are caused by representatives of a brackish, warm-water adapted globally distributed genotype (Tomas et al., 2012; Kremp et al., 2014). They differ from most of the other *A. ostenfeldii* isolates by their potential to produce PSP toxins in addition to or instead of spirolides and to potentially produce neurotoxic gymnodimines. This genotype has recently expanded within the northern Baltic Sea, a boreal cold-water system, presumably as result of increased summer surface temperatures (Kremp et al., 2009), and now regularly forms toxic blooms here. Most North Atlantic isolates, including subarctic strains from northern Iceland, though cluster in a different phylogenetic group and mainly produce spirolides. Spirolides are potent neurotoxins causing rapid death of mice when injected intraperitonally and are thus regarded as “emerging” toxins, even if the currently are not regarded as toxic tu humans and therefore not regulated.

Despite abundant records of *A. ostenfeldii* from arctic coasts, arctic populations have not been characterized in terms of phylogenetic affiliation and important phenotypic traits such as morphology, toxicity and allelopathic potency. Such information is important for assessing

111 the potential for bloom formation and risks of toxicity in a region where shellfish industry is
112 an important part of the local economy (Garcia, 2006). Here we present molecular,
113 morphological and physiological data of multiple *A. ostenfeldii* strains isolated from western
114 and southern Greenland and provide the first, to our knowledge, extensive phylogenetic and
115 morphological characterization as well as a detailed description of toxin profiles and lytic
116 capacity of arctic populations of this species.
117
118
119 **2. MATERIAL AND METHODS**
120
121 **2.1 Sampling and sample preparation**
122 A total of 36 clonal strains of *Alexandrium ostenfeldii* were established from water
123 samples collected at three stations at the west coast of Greenland (Fig. 1) during a cruise
124 aboard the research vessel “Maria S. Merian” in August 2012. Vertical net tows were
125 conducted at each station through the upper 30 m of the water column with a 20-µm-mesh
126 Nitex plankton net. Total volume of each net tow concentrate was measured and a 20 ml
127 subsample was fixed with paraformaldhyde (1% final concentration).
128 Seawater samples were taken at standard depths of 3, 8, and 20 m depth by means of 5 L
129 Niskin entrapment bottles mounted on a remotely triggered rosette-sampler. 50 mL water
130 sampes were fixed with neutral Lugol (2 % final concentration) in brown glass bottles.
131
132 **2.2 Plankton composition**
133 For a qualitative and quantitative characterization of the plankton community at the three
134 stations where *A. ostenfeldii* were isolated, both net tow and bottle samples were inspected
135 microscopically. For net tow concentrates, 0.5 mL of the PFA-fixed samples (corresponding

to 0.1 % of the entire net tow) was counted in small sedimentation chambers. From lugol-fixed Niskin bottle samples, 10 mL each for all three depths per station were settled in 10 mL settling chambers. Depending on the size and/or abundance of different categories these were counted in the whole chamber or in representative sub-areas. All counts were performed using an inverted microscope (Zeiss Axiovert 40C).

2.3 Cultures

Single cells of *Alexandrium* were isolated onboard from live net tow concentrates under a stereomicroscope (M5A, Wild, Heerbrugg, Switzerland) by micropipette. Single cells were transferred into individual wells of 96-well tissue culture plates (TPP, Trasadingen, Switzerland) containing 250 µL of K medium (Keller et al., 1987) prepared from 0.2 µm sterile-filtered natural Antarctic seawater diluted with seawater from the sampling location at a ratio of 1:10. Plates were incubated at 10°C in a controlled environment growth chamber (Model MIR 252, Sanyo Biomedical, Wood Dale, USA). After 3 to 4 weeks, unialgal isolates were transferred to 24-well tissue culture plates, each well containing 2 mL of K medium diluted 1:5 with Antarctic seawater. Exponentially growing isolates were finally used as inoculum for batch cultures in 65 mL polystyrene cell culture flasks and were maintained thereafter at 10° C under a photon flux density of 30-50 µmol m^{-2} s^{-1} on a 16:8 h light:dark photocycle in a temperature-controlled walk-in growth chamber. Different sets of cultures were maintained in K-medium and f/2 –Si enriched (Guillard and Ryther, 1962) sterilized filtered Baltic sea water adjusted to a salinity of 35. For all strains, species designation was confirmed by fluorescence microscopy of calcofluor-stained samples. All strains were analysed for toxins (PSP, spirolides and gymnodimines); lytic capacity was estimated for all but two strains which were lost before these analyses could be performed. Detailed morphometric analysis and molecular data were generated for 7 and 14 selected strains,

161 respectively (Table 1).

162

163 **2.4 DNA extraction and Phylogenetic analyses**

164 To determine the phylogenetic position of 14 selected Greenland strains and their ITS,
165 D1-D2 LSU and SSU rDNA sequences, cells were harvested from exponentially growing
166 cultures and their DNA was extracted and processed to sequencing as explained in detail in
167 Kremp et al. (2014). For ITS1 through D1-D2 LSU phylogenetic analysis, we used 14
168 sequences from Greenland together with 32 additional *A. ostenfeldii* strains obtained from
169 Genbank (Table S1) together with sequences of closely related *A. minutum* and *A. insuetum*.
170 For the SSU alignment (1684 bp) we used one strain from each sampling station and 67 SSU-
171 sequences of *A. ostenfeldii* and other *Alexandrium* species generated in this study or obtained
172 from Genbank (Table S1). The ITS-LSU sequences (1246 bp) and SSU sequences (1684 bp)
173 were aligned using MAFFT (Multiple Alignment with Fast Fourier Transform) (Katoh et al.,
174 2009), with default settings, as implemented in SeaView (Gouy et al., 2010). The resulting
175 alignments were deposited in a public web server ("PopSet" at ENTREZ), and will be
176 provided upon request.

177 Bayesian inferences (BI) were performed using the software MrBayes v3.2 (Ronquist
178 and Huelsenbeck, 2003) with the GTR+G substitution model (Rodriguez et al., 1990),
179 selected under the Bayesian Information Criterion (BIC) with jModelTest 0.1.1. (Posada,
180 2008). For priors, we assumed no prior knowledge on the data. Two runs of four chains (three
181 heated and one cold) were executed for $10x6^{15}$ generations, sampling every 500 trees. In each
182 run, the first 25% of samples were discarded as the burn-in phase. The stability of model
183 parameters and the convergence of the two runs were confirmed using Tracer v1.5 (Rambaut
184 and Drummond, 2007). Additionally, separate maximum likelihood phylogenetic trees based
185 on either ITS-LSU or SSU alignments were calculated in GARLI 2.0 (Zwickl, 2006) with

parameters estimated from the data, using an evolutionary model GTR+G, selected under the Akaike Information Criterion (AIC) with jModelTest 0.1.1. (Posada, 2008). Tree topology was supported with bootstrap values calculated with 1000 replicates.

2.5 Morphological characterization

For all strains, species designation was confirmed by fluorescence microscopy of calcofluor-stained samples. For a more detailed morphometric characterization of the Greenland isolates, 7 strains representing the 3 sampling stations were randomly chosen. For those, cell size measurements and plate observations were performed using light and epifluorescence microscopy. Cells were collected from exponentially growing cultures and preserved with 1-2% neutral Lugol's solution. To determine cell length and width, fixed cells were viewed under a Leica DMI3000B inverted microscope (Leica, Wetzlar, Germany) and photographed at 400x magnification with a Leica DFC 490 digital camera. Measurements were taken using the analysis tool of LAS (Leica Application Suite) camera software. Distinctive thecal plates were visualized under epifluorescence after applying a few drops of a 1 mg L^{-1} solution of Fluorescent Brightener 28 (Sigma-Aldrich). Evaluation of plate shapes (1' and s.a. plate) and plate measurements (1', s.a. and 6'') were carried out on images of cells photographed at 630 x magnification.

2.6 Toxin analyses

For toxin analysis, strains were grown in 65 mL plastic culture flasks at the standard culture conditions described above. For each harvest, cell density was determined by settling lugol fixed samples and counting >600 cells under an inverted microscope. Cultures at a cell density ranging from ranging from 400 - 5.000 cells mL^{-1} were harvested by centrifugation (Eppendorf 5810R, Hamburg, Germany) at 3220 g for 10 min, 50 mL for analyzing PSP

toxins and 15 mL for analysis of cyclic imines. Cell pellets were transferred to 1 mL microtubes, again centrifuged (Eppendorf 5415, 16,000 g, 5 min), and stored frozen (–20°C) until use.

Cyclic imine toxins including spirolides and gymnodimines (GYMs) were analyzed by liquid chromatography coupled to tandem mass spectrometry (MS^2). Mass spectral experiments were performed on an ABI-SCIEX-4000 Q Trap (Applied Biosystems, Darmstadt, Germany), equipped with a TurboSpray® interface coupled to an Agilent (Waldbronn, Germany) model 1100 LC. The LC equipment included a solvent reservoir, in-line degasser (G1379A), binary pump (G1311A), refridgerated autosampler (G1329A/G1330B), and temperature-controlled column oven (G1316A).

After injection of 5 µL of sample, separation of spirolides was performed by reversed-phase chromatography on a C8 column (50 × 2 mm) packed with 3 µm Hypersil BDS 120 Å (Phenomenex, Aschaffenburg, Germany) and maintained at 25 °C. The flow rate was 0.2 mL min^{-1} and gradient elution was performed with two eluents, where eluent A was water and eluent B was methanol/water (95:5 v/v), both containing 2.0 mM ammonium formate and 50 mM formic acid. Initial conditions were elution with 5% B, followed by a linear gradient to 100% B within 10 min and isocratic elution until 10 min with 100% B. The programme was then returned to initial conditions within 1 min followed by 9 min column equilibration (total run time: 30 min).

Mass spectrometric parameters were as follows: curtain gas: 20 psi, CAD gas: medium, ion spray voltage: 5500 V, temperature: 650°C, nebulizer gas: 40 psi, auxiliary gas: 70 psi, interface heater: on, declustering potential: 121 V, entrance potential: 10 V, exit potential: 22 V, collision energy: 57 V. Selected reaction monitoring (SRM) experiments were carried out in positive ion mode by selecting the transitions shown in Table 2. Dwell times of 40 ms were used for each transition.

Paralytic shellfish poisoning (PSP) toxins were analyzed by liquid chromatography with post-column derivatization and fluorescence detection as described in Suikkanen et al. (2012). Limits of quantification (s/n = 5) for the individual PSTs on column were as follows: GTX4: 1190 pg, GTX1: 1570 pg, GTX2: 63 pg, GTX3: 67 pg, STX: 61 pg, NEO: 585 pg, B1: 329 pg.

2.7 Estimation of lytic capacity

Isolates were screened for lytic activity by using a *Rhodomonas* bioassay (Tillmann et al., 2009). Clonal isolates of *A. ostenfeldii* were grown in batch cultures in 65 mL plastic culture flasks at standard culture conditions described above and were regularly inspected with a stereomicroscope. When cultures became dense (2.000-7.000 cells mL^{-1}) cell concentration of each strain was estimated by counting Lugol's iodine fixed cells within a subsample that contained at least 600 cells. Cultures were subsequently diluted with medium to a final cell concentration of approximately 1.000 cells mL^{-1}. Then 3.9 mL of diluted cultures was dispensed into triplicate 6 mL glass vials. Two negative and one positive control (triplicate each) were performed in the same way as the experimental assays. The first negative control contained only K medium (3.9 mL), whereas the second negative control was performed with *A. tamarense*, strain Alex5, a strain which previously was shown to be non-lytic (Tillmann and Hansen, 2009). The positive control was performed by adding 3.9 mL of a culture of the allelochemically active *A. tamarense* strain Alex 2 (Tillmann and Hansen, 2009). Each sample was spiked with 0.1 mL of a *Rhodomonas* culture which was adjusted (based on microscope cell counts) to 4×10^5 cells mL^{-1} yielding a final start concentration of 1×10^4 mL^{-1} of the target cells in the bioassay. Samples were then incubated for 24 h in the dark at 10°C. Subsequently, samples were fixed with 2% Lugol's iodine

261 solution and concentration of intact target cells was determined. All counts were performed
262 with an inverted microscope (Zeiss Axiovert 40C, Göttingen, Germany) in small counting
263 chambers with a volume set up for cell counts of 0.5 mL. A sub-area of the chamber
264 corresponding to at least 600 *Rhodomonas* cells in the control was counted. In order to
265 quantify lytic effects, only intact cells of the target species were scored. Strains of *A.*
266 *ostenfeldii* were simultaneously tested in groups of 3-10 strains in a total of 4 bioassay runs.
267 All results were expressed as final concentration of *Rhodomonas* expressed as percent of the
268 seawater control.
269
270
271 **3. RESULTS**
272
273 **3.1 Plankton situation**
274 We successfully isolated *Alexandrium ostenfeldii* from three stations located on the west
275 coast of Greenland (Fig. 1). At the northernmost station 506 located in the Uummannaq
276 Fjord, surface water of rather high temperature (5-7 °C) and low salinities (27-28) was
277 layered above cold (2 °C) and saline (32.7) water at 30 m depth. In contrast, at station 516
278 located south of Disco Island in the Disco Bay, salinity was constantly high (33.2-33.5) in the
279 upper 30 m. Surface temperature here was 6.8 °C in the upper 10 m and decreased steadily to
280 2.5 °C in 30 m. The lowest surface temperature was recorded at the southernmost station 524
281 (3.7 °C in the first 15 m, decreasing to 2.7 °C at 30 m depth) with salinity in the upper 30 m
282 ranging from 30.6 to 31.2.
283 Phytoplankton density at all three stations was generally low with chlorophyll values
284 ranging from 0.26 (Stat. 506, 30 m) to 2.0 µg L^{-1} (Stat 516, 20 m) with highest values at
285 depth of about 20 m (Daniela Voß, per. comm.). Plankton communities at the three stations

might be characterised as representing a post spring-bloom situation with relatively low biomass of photosynthesizing organisms and with a large and diverse proportion of heterotrophs (e.g tintinnids, aloricate ciliates, rotatoria, heterotrophic dinoflagellates).

At the northernmost station 506 there were some remains of the diatom bloom present, mainly species of *Thalassiosira*, large amounts of an unidentified small (<10 µm) diatom and some larger chain forming *Fragillaria* species. The most abundant species was the mixotrophic colony-forming chrysophyte *Dinobryon* sp. with up to 764 cells mL^{-1}. Photosynthetic dinoflagellets identified in net or Niskin sampes included *Dinophysis* spp., *Scrippsiella* sp. *Protoceratium reticulatum*, and *Gonyaulax* spp. A quite diverse assemblage of heterotrophic dinoflagellates including various species of the genus *Protoperidinium* was present.

The net tow sample of Station 516 was quite dilute and characterised by a variety of different dinoflagellate species with just a few diatom cells (*Cerataulina bergonii*, *Thalassiosira nordenskiöldii*, *Leptocylindrus* sp.) present. Most abundant in Niskin bottle samples were *Scrippsiella* sp. (17-30 mL^{-1}, range of three depth samples), *Protoperidinium* spp. (25-32 mL^{-1}) and ciliates (11-30 mL^{-1}), and unidentified small and medium-sized (10-30 µm) dinoflagellates (47-83 mL^{-1}). With densities up to 1216 mL^{-1} *Dinobryon* sp.was even more abundant compared to station 506.

Station 524 located at the southernmost tip of Greenland was distinctly different. The chrysophyte *Dinobryon* completely disappeared and the plankton was dominated by large amount of diatoms of the genus *Pseudonitzschia* (86-107 mL^{-1}) accompanied by some *Thalassiosira*. Most of the larger dinoflagellates were of the genus *Protoperidinium* with a few cells of *Dinophysis* spp., *Ceratium arcticum*, *C. fusus*, *Gonyaulax* spp. and *Protoceratium reticulatum* present.

The density of *Alexandrium* spp. at the three stations was generally low. Based on Niskin bottle samples, *Alexandrium* spp. (not determined at the species level) ranged between 0 and a maximum of 500 cells L^{-1} recorded at Station 516 (15 meter). Quantification of *Alexandrium* spp. in net tow samples indicated an abundance of 87 $x10^3$ (Stat 506) to 750 x 10^3 (Stat 524) cells per square meter in the upper 30 meter of the water column. At station 516 *A. ostenfeldii* co-occurred with *A. tamarense* and *A. tamutum*, as all three species were successfully isolated from the same sample (to be reported elsewhere). In contrast, all *Alexandrium*-like cells isolated from station 524 and successfully brought into culture turned out to be *A. ostenfeldii*. Many of the *Alexandrium* cells observed in net tow sample from station 524 contained large inclusion (Fig. 2).

3.2 Phylogenetic position of Greenland isolates

All of the selected 14 strains from the 3 sampling stations had identical ITS, LSU and SSU sequences. Bayesian Inference (BI) and Maximum Likelihood (ML) methods returned identical tree topologies for ITS-LSU data set (Fig. 3). In the phylogenetic tree, Greenland *Alexandrium* strains from all 3 stations grouped together with each other and with strains from Iceland and the Gulf of Maine (USA), constituting a well-supported monophyletic (ML 99 %, BI 1.0) clade, consistent with group 5 defined by Kremp et al. (2014). BI and ML analyses of SSU sequences (supplementary figure S1) showed a different, more conserved tree topology, where *A. ostenfeldii* was not grouped into 6 different groups as based on ITS and LSU sequences, but into three major groups. The first group collates groups 1 and 2 of the ITS-LSU phylogeny, placing strains from the Baltic Sea, US East coast estuaries and China in the same cluster with isolates from the UK, Ireland and Spain (ML 90 %, BI 0.93). The second group (ML 82 %, BI 0.99) is identical with group 6 of the ITS-LSU phylogeny and a third group (ML 55 %, BI 0.56) combines ITS-LSU groups 3, 4 and 5. Here again, the

Greenland isolates are most similar to strains from the NW Atlantic, and appear slightly differentiated from the Japanese (ML 82 %, BI 100) and New Zealand populations (ML 83 %, BI 100).

3.3 Morphology

Cells of *Alexandrium ostenfeldii* from Greenland were round to ellipsoid in shape (Fig. 4 A, B). Mean cell size varied among the examined strains with largest cells (mean cell length = 45.78 ±6.47) found in strain P1H10 and smallest cells found in P1D5 (28.83 (±2.41). Most strains were of medium size with mean cell lengths of 33 to 37 µm (Table 3). With mean width to height ratios of 0.89- 0.97, the majority of the examined strains were slightly longer than wide (Table 3). Most round cells were found in strain P1F8, while cells were particularly elongated in strain P2G3.

Dimensions of plates varied among strains, largest 1' plates were found in the largest cells (strain P1H10) (Table 3). Most of the examined strains had narrow 1' plates (Fig. 4 B, C), with the angular shape and the large ventral pore typical for *A. ostenfeldii*. The right anterior margins of cells from Greenland strains were mostly straight with a few cases where curved or irregular margins were detected (Table 3, Fig. 4 C, E). Two of the 7 analyzed strains, P1H10 and P2G3 had a significant amount of cells whose 1' plate was anteriorly extended. Except for strain P2G3, which contained a significant amount of cells with A-shaped s.a. plates, the vast majority of examined cells from the investigated strains had door-latch-shaped s.a. plates (Table 3, Fig. 4 B, D, E). Commonly, a fold was observed on these plates (Fig. 4 E). Width to height ratios of the anterior sulcal plate (s.a.) revealed that these plates were generally lower than high (Table 3). This was also the case for the 6'' plate (Table 3, Fig. 4 E). Generally the variability in w/h measurements of the s.a. and 6'' plates was high as indicated by high standard deviations. The pore plate with the comma-shaped

apical pore (Fig. 4 G) and the sulcal plates (Fig. 4 H) showed the typical shapes and arrangements of *Alexandrium ostenfeldii*.

3.4 Toxin composition

All the 36 analyzed strains were spirolide producers, but none of them produced gymnodinime A (GYM-A), 12-methyl GYM-A or paralytic shellfish poisoning (PSP) toxins. The limits of detection (LODs) for PSP toxins expressed as cell quotas are quite variable depending on the different sensitivities of individual PSP toxins and the varying amounts of cells used for analysis (depending on the growth of individual strains). The lowest LOD was 0.005 pg $cell^{-1}$ of the most sensitive GTX-2 for strain P3F1with most harvested cells and the highest LOD was 8.4 pg $cell^{-1}$ of the least sensitive GTX-1 for strain P2F3 with the lowest number of harvested cells.

Spirolide compositions among strains were very diverse (Table 4), however, the most frequent spirolides were spirolide C and 20-methyl spirolide G. Even though no standards for spirolide C and 20-methyl spirolide G are available, their product ion spectra are well documented in the literature (Hu et al., 2001; Aasen et al., 2005) and they could be identified by the comparison of collision induced dissociation (CID) product ion spectra. In addition, spirolide H (Roach et al., 2009) was also identified by CID spectra comparison. The fourth spirolide unambiguously identified was 13-desmethyl spirolide C, which is the only spirolide for which a standard is commercially available. Besides these four spirolides, there were eight other compounds with CID spectra characteristic for spirolides, i.e. the cyclic imine fragments m/z 150, 164 or 180 and the formation of the “F1” fragment (Sleno et al., 2004), which is formed by a retro-Diels-Alder reaction and the cleavage of a C_{15}-element including the lactone moiety. These putative spirolides could not unambiguously be assigned or they have not been reported in the literature yet. For molecular masses and CID spectra see

supplementary material. Spirolide profiles of strains isolated from station 524 were similar and spirolides C and 20-methyl G in all strains from this station made up more than 90% of total spirolides. In contrast, spirolide composition and abundances were more diverse among strains isolated from station 516 (Tab. 4). Spirolide cell quotas ranged from very low levels of 0.02 pg cell^{-1} up to 66 pg cell^{-1} (data not shown).

3.5 Lytic activity

Screening for lytic capacity performed at one cell density of approximately 1000 cells (685-1300, mean = 941, SD = 115) indicates that with one exception (see below), all strains of *A. ostenfeldii* at that concentration clearly had the capacity to lyse the target *Rhodomonas salina* (Fig. 5). In all bioassay runs, positive controls (using the known lytic *A. tamarense* strain Alex2) yielded total lysis of *Rhodomonas*, whereas in all negative controls using the non-lytic strain Alex5 were not sigificantly different from seawater controls (data not shown). At the fixed dose of ca. 1000 cells mL^{-1}, lytic capacity varied considerably with the final number of intact *Rhodomonas* ranging from 0 to 92%. When tested with a simple t-test, final *Rhodomonas* concentration incubated with strain P1G6 was not significantly different to the control. An additional test of strain P1G6 tested at a distinctly higher dose (ca. 3000 cells mL^{-1}) clearly showed that this strain is lytic as well (result not shown).

4. DISCUSSION

Recent phylogenetic investigations of the *Alexandrium ostenfeldii* species complex (including *A. peruvianum*) revealed that global isolates are genetically differentiated into 6 groups (Kremp et al. 2014). In the respective concatenated ITS-LSU phylogeny, these groups

410 fall into two major clusters, one consisting groups 1 and 2 which contain a mix of geographic
411 isolates from shallow estuarine, often brackish habitats, and the other one containing
412 geographically differentiated Groups 3 to 6. The ITS-LSU analysis performed in the present
413 study reproduced the Kremp et al. (2014) phylogeny and identified the Greenland isolates as
414 members of Group 5, representing *A. ostenfeldii* populations from the western coasts of the
415 North Atlantic. Also in the SSU phylogeny, Group 5 strains, including the representative
416 Greenland isolates grouped together, however, with this more conserved marker, the groups
417 were not as well resolved. Group 5 strains are nested in a cluster together with Group 3 and 4
418 isolates from New Zealand and Japan. SSU analysis emphasize the close relationship of
419 Group 1 and 2 strains suggested by morphological and physiological similarities found earlier
420 (Kremp et al., 2014): the two groups appear collated when compared with the more
421 conserved SSU marker (suppl. Figure S1).

422 The morphological characters found in the Greenland isolates are consistent with their
423 molecular identity and placement in Group 5. The typically longer than wide cells from the
424 Greenland material mostly exhibited narrow 1' plates, door-latch shaped s.a. plates and low
425 6'' plates, features which are most commonly found in the closest genetic and geographic
426 neighbors from the Gulf of Maine, Atlantic Canada and Northern Iceland (Kremp et al.,
427 2014). Cell dimensions, plate shapes and w/h measurements of the s.a. and 6'' plates varied
428 somewhat among the studied strains, as typical for *A. ostenfeldii*. Mean cell length was
429 generally smaller than reported from field material (Balech and Tangen, 1985; Gribble et al.,
430 2005) but cell size measurements of the Greenland strains were on average comparable to
431 other cultured Group 5 isolates (Kremp et al., 2014). It has been suggested earlier that
432 cultured cells of *A. ostenfeldii* are generally smaller than in their natural environment (John et
433 al., 2003).

Though the geographic distance between the Greenland population and other Group 5 isolates is considerable, the Greenland strains very likely represent a natural extension of this group into the western Subarctic and Arctic. *A. ostenfeldii* has been reported from the northern St Lawrence Estuary (Levasseur et al., 1998). Sequence data is not available from this location, but likely these occurrences extend the Gulf of Maine and Nova Scotia populations. Being present in the northern Gulf of St Lawrence which opens to the North Atlantic, *A. ostenfeldii* is exposed here to the Subpolar Gyre, which connects the eastern coast of North America with the coasts of Greenland and Iceland. Group 5 representatives generally seem to thrive in marine cold-water environments: A study on the Gulf of Maine and Nova Scotia isolates showed that growth rates were higher at 10 degrees than at 15 degrees (Cembella et al., 2000b; Cembella et al., 2000a). Gribble et al. (2005) found that the numbers of *A. ostenfeldii* cells decreased in the water column as water temperatures increased in late spring. Generally, *A. ostenfeldii* is widely distributed in cold water environments such as the Russian Arctic (Okolodkov, 2005), and often reported from spring phytoplankton communities (Paulsen, 1904; Balech and Tangen, 1985; Moestrup and Hansen, 1988; Levasseur et al., 1998) emphasizing that a cold-water ecotype of this species commonly occurs. The observations of cold water occurrences of *A. ostenfeldii* in the Gulf of Maine, Atlantic Canada and Iceland (Paulsen, 1904), suggests that Group 5 represents this cold water ecotype. In the present study we do not systematically address the ecological preferences of the Greenland isolates, but it can be noted that most isolates grow better when maintained at 11 °C compared to 16 °C (J. Oja, personal communication) suggesting that they are adapted to cooler rather than warmer water.

Large toxic blooms have so far mostly been related with Group 1 genotypes. Recently, blooms of this genotype have been expanding in brackish US east coast estuaries, river estuaries of Western Europe and in the Baltic Sea (Hakanen et al., 2012; Tomas et al., 2012;

Burson et al., 2014). Because of the clustering of the Greenland isolates in cold-water adapted phylogenetic Group 5, a comparable temperature related expansion of *A. ostenfeldii* is not expected in Greenland.Group 1 differs physiologically from Group 5 by being adapted to low salinities and thriving in warm water. In contrast to Group 5, Group 1 *A. ostenfeldii* produces paralytic shellfish toxins (PST's) in addition to or instead of spirolides and gymnodimines and blooms are of concern because they are associated with high PST concentrations in the water (Burson et al., 2014).

Consistent with the Group 5 isolates investigated earlier, only spirolides were detected in the 36 Greenland isolates analyzed here for toxin composition. Particularly *A. ostenfeldii* from Groups 2, 4 and 5 seem to lack the ability to produce PSTs and gymnodimines due to complete or partial absence of the respective genes (Suikkanen et al., 2013). A particularly striking feature of the Greenland isolates is the high diversity of spirolide analogues. To date 14 different spirolides are known (Molgó et al., 2014), but spirolide diversity in *A. ostenfeldii* seems to be higher, as the Greenland isolates apparently produce at least 8 spirolides not reported in the literature. This lack of knowledge has two reasons; 1) spirolides do not belong to regulated shellfish toxins and accordingly there is no economically driven interest in research into this field and 2) spirolides are large molecules with many options for slight modifications such as hydroxylation, hydration/dehydration or methylation, which may and apparently do result in many analogs of the same structural body. These modifications may be introduced by slight modifications of the synthesing enzymes over evolutionary times and is observed in other toxin classes as well.

The few available studies on spirolide composition also suggest that spirolide variability in *A. ostenfeldii* is generally high. On one hand already 14 different spirolides haven been comprehensively described and structurally elucidated from strains of different geographic locations (Molgó et al., 2014). On the other, Gribble et al. (2005) detected up to 7 different

spirolides and found high spirolide variation among 15 strains of *A. ostenfeldii* from the Bay of Fundy, North West Atlantic, a geographically very constrained area. Our findings (12 different spirolides in 36 strains from 3 stations) confirm this pattern. The CID spectrum of compound 2 (Fig. S2F) is consistent with spirolide A, but due to lack of any reference material an unambiguous identification is not possible. Compound 1 (Fig. S2E) has a 14 Da smaller molecular ion than compound 2 and thus may be a yet unreported desmethyl spirolide A. Interestingly there were three compounds with the molecular mass of m/z 722 present. (Figs. S2J, K, and L). Compound 6 instead of the commonly observed cyclic imine fragments of m/z 150 or 164 showed a fragment of m/z 180, which for the first time was described for 27-hydroxy-13-desmethyl spirolide C by Ciminiello et al. (2010). The CID spectrum of compound 6 with a 14 Da higher molecular mass than 27-hydroxy-13-desmethyl spirolide C is consistent with 27-hydroxy spirolide C; however, these are only hypothetical structures which have to be confirmed by NMR. In addition there are spirolides with unusual molecular masses such as compound 4 (m/z 696) and compound 5 (m/z 720) (Figs. S2H and I). The fact that of the 12 spirolides detected in the Greenland isolates described here, 8 are yet undescribed or at least not unambiguously attributed to known spirolides, highlights the need for further research in this field

We estimated the cell quota of total spirolide content to be ranging from very low levels of 0.02 pg cell^{-1} up to 66 pg cell^{-1}. Although cultures were grown under identical environmental conditions, strains considerably differed (although not quantified) in growth performance and cell yield. Cultures were thus not harvested at the same growth stages and/or cell density and this may have partly influenced spirolide cell quota. Cell quota for one strain of *A, ostenfeldii* from Canada has been described to vary almost ten-fold depending on environmental condition, ranging from ca. 30 to 240 pg cell^{-1} (Maclean et al., 2003) For 20 of the 36 Greenland strains we estimated a cell quota of less than 1 pg per cell which is

509 rather low compared to these literature values. Cell quota of field samples have been shown
510 to be quite variable as well ranging from 168 pg per cell to no detectable spirolides despite
511 rather high concentrations of *A. ostenfeldii* (Gribble et al., 2005). Cell quotas of 1 to 60 pg
512 per cell estimated for 16 Greenland strains are well in the range of other studies where cell
513 quotas of about 6 to 66 pg per cell are reported (Cembella et al., 2000a; Gribble et al., 2005;
514 Tatters et al., 2012).

515 In addition to the production of spirolide toxins, all strains of *A. ostenfeldii* from
516 Greenland produce alleochemicals with the capacity to lyse cells of the target species
517 *Rhodomonas*. Lytic activity of extracellular secondary metabolites is rather widespread in the
518 genus *Alexandrium* and has been shown to affect other microalgae (Arzul et al., 1999;
519 Tillmann et al., 2008), heterotrophic protists (Hansen et al., 1992; Matsuoka et al., 2000;
520 Tillmann and John, 2002) and microbial communities (Weissbach et al., 2011). Deleterious
521 effects in particular of *A. ostenfeldii* on other microorganisms have been known for a long
522 time. Hansen et al. (1992) described cell lysis of tintinnid predators of a Danish isolate of *A.*
523 *ostenfeldii* in culture experiments, which they – at that time – discussed as potentially related
524 to the PSP toxin content of that *A. ostenfeldii* strain. Although molecular structures and exact
525 mode of action of allelochemicals from *Alexandrium* still are poorly known (Ma et al., 2009;
526 Ma et al., 2011) it is now clear that they are unrelated to the known toxins produced by this
527 genus (Tillmann and John, 2002; Tillmann et al., 2007). In the latter paper, three strains of *A.*
528 *ostenfeldii* from different geographic origin and with or without spirolides all showed
529 deleterious effects on a number of prostistan species. There are indications that isolates of *A.*
530 *ostenfeldii* from other areas are lytic as well: haemolytic activity has been described for
531 *Alexandrium peruvianum* (= *A. ostenfeldii*) from coastal waters of North Carolina (Tatters et
532 al., 2012; Tomas et al., 2012) and production of allelochemicals has been shown for isolates
533 of *A. ostenfeldii* from the Baltic Sea which deter copepod grazers by unknown chemical

534 substances (Sopanen et al., 2011), and negatively affect co-occurring phytoplankton
535 (Hakanen et al., 2014).

536 We used a simple one-concentration bioassay to show lytic activity and we do not yet
537 have full dose-response curves that are needed to estimate EC_{50} (cell concentration of *A.*
538 *ostenfeldii* causing lysis of 50% of the *Rhodomonas* population) values. Nevertheless, our
539 data show that EC_{50} values of most Greenland isolates grown at 10 °C seem to be well below
540 1000 cells mL^{-1} and would thus be in the range of EC_{50} value estimated for temperate
541 isolates, which have been shown to range from 0.3 to 1.9 x 10^3 cells mL^{-1} (Tillmann et al.,
542 2007). This is in the range of values determined for Baltic isolates (Hakanen et al., 2014),
543 suggesting similar lytic capacities in the different phylogenetic groups of *A. ostenfeldii*. EC_{50}
544 values for hemolyis of *A. ostenfeldii* from the US coast given by Tomas et al. (2012) and
545 Tatters et al. (2012) for the same strain, seem to be orders of magnitude higher but refer to
546 different target cells and procedures than used in standard assays.

547 Our screening also indicates that there are profound quantitative differences in lytic
548 activity between different isolates. It has to be kept in mind that our strains were grown at
549 exactly the same environmental conditions but have not been sampled at a defined growth
550 stage, which might have contributed to the observed strain differences. Quantitative
551 differences in lytic activity within a population of *Alexandrium* have been described before
552 for isolates of *A. tamarense* from the northern North Sea (Alpermann et al., 2010). Such a
553 high phenotypic variability, also manifested here in the high variability in the spirolide
554 profile with *A. ostenfeldii* from Greenland, and manifested in the North Sea population of *A.*
555 *tamarense* by a high strain variability in PSP toxin profile, has been discussed as evidence for
556 lack of strong selective pressure on respective phenotypic traits at the time the population
557 was sampled (Alpermann et al., 2010).

Lytic effects at cell concentrations used in this study were almost three orders of magnitude above the densities of *Alexandrium* spp. estimated in the field samples during our field expedition. Nevertheless, motile phytoplankton, such as *Alexandrium* spp, may accumulate in horizontal layers under certain conditions, along thermoclines or the water surface (MacIntyre et al., 1997; Mouritsen and Richardson, 2003) and the resulting high densities may be accompanied by effective concentrations of secondary metabolites in these layers

Lytic compounds produced by *A. ostenfeldii* may be involved in cell-to-cell interactions, e.g. in prey capture. A number of allelochemically active microalgae, including species of *Alexandrium* and *A. ostenfeldii*, have been shown to be mixotrophic (Jacobson and Anderson, 1986; Tillmann, 1998; Jeong et al., 2005; Stoecker et al., 2006; Yoo et al., 2009; Sheng et al., 2010; Blossom et al., 2012) and it has been speculated that allelochemicals are used for predation. Large food vacuoles, as observed here for most of the specimen at station 524 (Fig. 2) have been described for *A. ostenfeldii* for a number of field sample sites (Jacobson and Anderson, 1986; Gribble et al., 2005). In our experiments, however, we did not observe any particulate uptake of *Rhodomonas* by *A. ostenfeldii* and clearly more detailed experiments are needed to clarify mixotrophy in *A. ostenfeldii* and a potential role of lytic activity in prey capture.

To conclude, spirolide producing and lytic *A. ostenfeldii* are present along the west coast of Greenland. In accordance with the phylogenetic analysis, the arctic cold water population, however, does not produce PSP toxins and thus does not contribute to the PSP toxicity in the region (Baggesen et al., 2012) which is thus probably caused exclusively by *A. tamarense*. Spirolides currently are not considered dangerous to humans at the concentrations found in shellfish and are therefore not regulated, but they clearly are potent neurotoxins causing rapid death of mice when injected intraperitoneally. Furthermore, they were found to be toxic to

583 mice in oral feeding studies, and are therefore regarded as so-called “emerging” toxins. Our
584 results show the presence of numerous new spirolide analogs whose specific toxicity
585 currently is unknown. Low cell concentrations of *A. ostenfeldii* as found in plankton samples
586 during our summer cruise and the preference for cold water where slow growing
587 dinoflagellates are usually outcompeted by fast growing diatoms, does not exclude the
588 possibility that this species may, under certain circumstances, form blooms. An increase of
589 dinoflagellate proportions and dinoflagellate dominated blooms has been reported from other
590 cold-water systems (Klais et al., 2011). In the Baltic Sea, the recent increase of dinoflagellate
591 spring blooms has been related to favourable effects of changing climate conditions on the
592 recruitment of the respective species from their cyst beds, which provides them a competitive
593 advantage over diatoms (Kremp et al., 2008; Klais et al., 2011). Also *A. ostenfeldii* forms
594 resting cysts (Mackenzie et al., 1996) and hence the seasonal dynamics may largely depend
595 on cyst germination and formation processes that are potentially influenced by changing
596 environmental conditions. In fact, cysts of *Alexandrium* have been detected in West
597 Greenland sediments (Mindy Richlen, pers. com). It is not known whether life cycle
598 regulated indirect effects of bloom promotion could eventually also favour cold-water *A.*
599 *ostenfeldii* in coastal waters of western Greenland. Further field studies and ecophysiological
600 experiments targeting the life cycle, growth performance and toxin production at different
601 environmental conditions are now needed to estimate the impact of global change and
602 temperature increase on the survival, establishment, extension, and bloom formation of
603 *Alexandrium* spp. and to fully evaluate the risk potential of algal toxins for arctic regions with
604 shellfish industry as an important and rising part of the local economy.
605
606
607 **ACKNOWLEDGEMENTS**

608 Thanks to Captain Bergmann and the FS Maria S. Merian crew for their assistance and
609 support for the collection of field material. Financial support was provided by the PACES
610 research program of the Alfred Wegener Institute as part of the Helmholtz Foundation
611 initiative in Earth and Environment.

612 **REFERENCES**

613

614 Aasen, J., MacKinnon, S.L., LeBlanc, P., Walter, J.A., Hovgaard, P., Aune, T., Quilliam, M.A.,
615 2005. Detection and Identification of Spirolides in Norwegian Shellfish and
616 Plankton. Chemical Research in Toxicology 18, 509-515
617 Alcaraz, M., Felipe, J., Grote, U., Arashkevich, E., Nikishina, A., 2014. Life in a warming
618 ocean: thermal thresholds and metabolic balance of arctic zooplankton. J.
619 Plankton Res. 36, 3-10
620 Alpermann, T.J., Tillmann, U., Beszteri, B., Cembella, A.D., John, U., 2010. Phaenotypic
621 variation and genotypic diversity in a planktonic population of the toxigenic
622 marine dinoflagellate *Alexandrium tamarense* (Dinophyceae). J. Phycol. 46, 18-32
623 Anderson, D.M., Alpermann, T.J., Cembella, A.D., Collos, Y., Masseret, E., Montresor, M.,
624 2012. The globally distributed genus *Alexandrium*: multifaceted roles in marine
625 ecosystems and impacts on human health. Harmful Algae 14, 10-35
626 Arzul, G., Seguel, M., Guzman, L., Erard-LeDenn, E., 1999. Comparison of allelopathic
627 properties in three toxic *Alexandrium* species. J. Exp. Mar. Biol. Ecol. 232, 285-
628 295
629 Baggesen, C., Moestrup, Ø., Daugbjerg, N., Krock, B., Cembella, A.D., Madsen, S., 2012.
630 Molecular phylogeny and toxin profiles of *Alexandrium tamarense* (Lebour)
631 Balech (Dinophyceae) from the west coast of Greenland. Hamful Algae 19, 108-
632 116
633 Balech, E., 1995. The Genus *Alexandrium* Halim (Dinoflagellata). Sherkin Island Marine
634 Station, Sherkin Island Co, Cork, Ireland.
635 Balech, E., Tangen, K., 1985. Morphology and taxonomy of toxic species in the
636 tamarensis group (Dinophyceae): *Alexandrium excavatum* (Braarud) *comb. nov.*
637 and *Alexandrium ostenfeldii* (Paulsen) *comb. nov.* Sarsia 70, 333-343
638 Blossom, H., Daugbjerg, N., Hansen, P.J., 2012. Toxic mucus traps: A novel mechanism
639 that mediates prey uptake in the mixotrophic dinoflagellate *Alexandrium*
640 *pseudogonyaulax*. Harmful Algae 17, 40-53
641 Brown, L., Bresnan, E., Graham, J., Lacaze, J.P., Turrell, E., Collins, C., 2010. Distribution,
642 diversity and toxin composition of the genus *Alexandrium* (Dinophyceae) in
643 Scottish waters. Eur. J. Phycol. 45, 375-393
644 Burson, A., Matthijs, H.C.P., de Bruijne, W., Talens, R., Hoogenboom, R., Gerssen, A.,
645 Visser, P.M., Stomp, M., Steur, K., van Scheppingen, Y., Huisman, J., 2014.
646 Termination of a toxic *Alexandrium* bloom with hydrogen peroxide. Hamful Algae
647 31, 125-135
648 Cembella, A.D., Lewis, N.I., Quilliam, M.A., 2000a. The marine dinoflagellate *Alexandrium*
649 *ostenfeldii* (Dinophyceae) as the causative organism of spirolide shellfish toxins.
650 Phycologia 39, 67-74
651 Cembella, A.D., Bauder, A.G., Lewis, N.I., Quilliam, M.A., 2000b. Population dynamics and
652 spirolide composition of the toxigenic dinoflagellate *Alexandrium ostenfeldii* in
653 coastal embayments of Nova Scotia. In: Hallegraeff, G.M., Blackburn, S.I., Bolch,
654 J.S., Lewis, R.J. Eds. Proceedings of the IX International Conference on Harmful
655 Algal Blooms. Intergovernmental Oceanographic Commission, Hobart, Australia,
656 pp 173-176
657 Ciminiello, P., Dell'Aversano, C., Fattorusso, E., Magno, S., Tartaglione, L., Cangini, M.,
658 Pompei, M., Guerrini, F., Boni, L., Pistocchi, R., 2006. Toxin profile of *Alexandrium*

659 *ostenfeldii* (Dinophyceae) from the Northern Adriatic Sea revealed by liquid
660 chromatography-mass spectrometry Toxicon 47,
661 Ciminiello, P., Dell'Aversano, C., Dello Iacovo, E., Fattorusso, E., Forino, M., Grauso, L.,
662 Tartaglione, L., Guerrini, F., Pezzolesi, L., Pistocchi, R., 2010. Characterization of
663 27-hydroxy-13-desmethyl spirolide C and 27-oxo-13,19-didesmethyl spirolide C.
664 Further insights into the complex Adriatic *Alexandrium ostenfeldii* toxin profile.
665 Toxicon 56, 1327-1333
666 Comiso, J.C., Parkinson, C.L., Gersten, R., al., e., 2008. Accelerated decline in the Arctic sea
667 ice cover. Geophys. Res. Lett. 35, L01703
668 Fraga, S., Sanchez, F.J., 1985. Toxic and potentially toxic dinoflagellates found in Galician
669 Rias (NW Spain). In: Anderson, D.M., White, A.W., Baden, D.G. Eds. Toxic
670 Dinoflagellates. Elsevier-North Holland, New York, pp 51-54
671 Garcia, V.M.T., 2006. Probable origin and toxin profile of *Alexandrium tamarense*
672 (Lebour) Balech from southern Brazil. Harmful Algae 5, 36-44
673 Gouy, M., Guindon, S., Gascuel, O., 2010. SeaView version 4: a multiplatform graphical
674 user interface for sequence alignment and phylogenetic tree building. Mol. Biol.
675 Evol. 27, 221-224
676 Gribble, K.E., Keafer, B.A., Quilliam, M.A., Cembella, A.D., Kulis, D.M., Manahan, A.,
677 Anderson, D.M., 2005. Distribution and toxicity of *Alexandrium ostenfeldii*
678 (Dinophyceae) in the Gulf of Maine, USA. Deep Sea Research Part II: Topical
679 Studies in Oceanography 52, 2745-2763
680 Guillard, R.R.L., Ryther, J.H., 1962. Studies on marine planktonic diatoms. I. *Cyclotella*
681 *nana* Hustedt and *Detonula confervaceae* (Cleve) Gran. Can. J. Microbiol. 8, 229-
682 239
683 Hakanen, P., Suikkanen, S., Kremp, A., 2014. Intra-population variability in allelopathic
684 activity of the bloom-forming *Alexandrium ostenfeldii* and response of co-
685 occurring dinoflagellates. Harmful Algae , in press,
686 Hakanen, P., Suikkanen, S., Franzén, J., Franzén, H., Kankaanpää, H., Kremp, A., 2012.
687 Bloom and toxin dynamics of *Alexandrium ostenfeldii* in a shallow embayment at
688 the SW coast of Finland, northern Baltic Sea. Hamful Algae 15, 91-99
689 Hallegraeff, G.M., 1993. A review of harmful algal blooms and their apparent global
690 increase. Phycologia 32, 79-99
691 Hallegraeff, G.M., 2010. Ocean climate change, phytoplankton community responses,
692 and harmful algal blooms: a formidable predictive challenge. J. Phycol. 46, 220-
693 235
694 Hansen, P.J., Cembella, A.D., Moestrup, Ø., 1992. The marine dinoflagellate *Alexandrium*
695 *ostenfeldii*: paralytic shellfish toxin concentration, composition, and toxicity to a
696 tintinnid ciliate. J. Phycol. 28, 597-603
697 Hu, T., Burton, I.W., A.D., C., Curtis, J.M., Quilliam, M.A., Walter, J.A., Wright, J.L.C., 2001.
698 Characterization of Spirolides A, C, and 13-Desmethyl C, new marine toxis
699 isolated from toxic plankton and contaminated shellfish. J. Nat. Prod. 65, 308-312
700 Jacobson, D.M., Anderson, D.M., 1986. Thecate heterotrophic dinoflagellates: feeding
701 behaviour and mechanisms. J. Phycol. 22, 249-258
702 Jeong, H.J., Yoo, Y.D., Park, J.Y., Song, J.Y., Kim, S.T., Lee, S.H., Kim, K.Y., Yih, W.H., 2005.
703 Feeding by phototrophic red-tide dinoflagellates: five species newly revealed
704 and six species previously known to be mixotrophic. Aquat. Microb. Ecol. 40,
705 133-150
706 John, U., Cembella, A.D., Hummert, C., Elbrächter, M., Groben, R., Medlin, L., 2003.
707 Discrimination of the toxigenic dinoflagellates *Alexandrium tamarense* and *A.*

ostenfeldii in co-occurring natural populations from Scottish coastal waters. Eur. J. Phycol. 38, 25-40

Katoh, K., Asimenos, G., Toh, H., 2009. Multiple alignment of DNA sequences with MAFFT. Method. Mol. Biol. 537, 39-64

Keller, M.D., Selvin, R.C., Claus, W., Guillard, R.R.L., 1987. Media for the culture of oceanic ultraphytoplankton. J. Phycol. 23, 633-638

Klais, R., Tamminen, T., Kremp, A., Spilling, K., Olli, K., 2011. Decadal-scale changes of dinoflagellates and diatoms in the anomalous Baltic Sea spring bloom. PLOSOne 6, e21567

Konovalova, G.V., 1991. The morphology of *Alexandrium ostenfeldii* (Dinophyta) from littoral waters of eastern Kamchatka. Botanichyeskii Zhurnal (Leningrad) 76, 79-94

Kremp, A., Tamminen, T., Spilling, S., 2008. Dinoflagellate bloom formation in natural assemblages with diatoms: Nutrient competition and growth strategies in spring bloom experiments in the Northern Baltic Sea. Aquat. Microb. Ecol. 50, 181-196

Kremp, A., Lindholm, T., Dreßler, N., Erler, K., Gerds, G., Eirtovaara, S., Leskinen, E., 2009. Bloom forming *Alexandrium ostenfeldii* (Dinophyceae) in shallow waters of the Aland Archipelago, Northern Baltic Sea. Harmful Algae 8, 318-328

Kremp, A., Godhe, A., Egardt, J., Dupont, S., Suikkanen, S., Casabianca, S., Penna, A., 2012. Intraspecific variability in the response of bloom forming marine microalgae to changing climatic conditions. Ecol. Evol. 2, 1195-1207

Kremp, A., Tahvanainen, P., Litaker, W., Krock, B., Suikkanen, S., Leaw, C.P., Tomas, C., 2014. Phylogenetic relationships, morphological variation, and toxin pattern in the *Alexandrium ostenfeldii* (Dinopyhceae) complex: implications for species boundaries and identities. J. Phycol. 50, 81-100

Kwok, R., Rothrock, D.A., 2009. Decline in Arctic sea ice thickness from submarine and ICESatr records: 1958–2008. Geophys. Res. Lett. 36, L15501

Levasseur, M., Berard-Therriault, L., Bonneau, E., Roy, S., 1998. Distribution of the toxic dinoflagellate *Alexandrium ostenfeldii* in the Gulf of St. Lawrence, Canada. In: Reguerra, B., Blanco, J., Fernández, M.L., Wyatt, T. Eds. Proceedings of the VIII International Conference on Harmful Algae. Xunta de Galacia, Intergovernmental Oceanographic Commission of UNESCO, Vigo, Spain, pp 54–57

Lilly, E.L., Halanych, K.M., Anderson, D.M., 2007. Species boundaries and global biogeography of the *Alexandrium tamarense* species complex. J. Phycol. 43, 1329-1338

Ma, H., Krock, B., Tillmann, U., Cembella, A., 2009. Preliminary characterization of extracellular allelochemicals of the toxic marine dinoflagellate *Alexandrium tamarense* using a *Rhodomonas salina* bioassay. Mar. Drugs 7, 497-522

Ma, H., Krock, B., Tillmann, U., Muck, A., Wielsch, N., Svatos, A., Cembella, A., 2011. Isolation of activity and partial characterization of large non-proteinaceous lytic allelochemicals produced by the marine dinoflagellate *Alexandrium tamarense*. Harmful Algae 11, 65-72

MacIntyre, J.G., Cullen, J.J., Cembella, A.D., 1997. Vertical migration, nutrition and toxicity in the dinoflagellate *Alexandrium tamarense*. Mar. Ecol. Prog. Ser. 148, 201-216

Mackenzie, L., White, D., Oshima, Y., Kapa, J., 1996. The resting cysts and toxicity of *Alexandrium ostenfeldii* (Dinophyceae) in New Zealand. Phycologia 35, 148-155

Maclean, C., Cembella, A.D., Quilliam, M.A., 2003. Effects of light, salinity and inorganic nitrogen on cell growth and spirolide production in the marine dinoflagellate *Alexandrium ostenfeldii* (Paulsen) Balech *et* Tangen. Bot. Mar. 46, 466-474

757 Matsuoka, K., Cho, H.J., Jacobson, D.M., 2000. Observation of the feeding behaviour and
758 growth rates of the heterotrophic dinoflagellate *Polykrikos kofoidii*
759 (Polykrikaceae, Dinophyceae). Phycologia 39, 82-86
760 Moestrup, Ø., Hansen, P.J., 1988. On the occurrence of the potentially toxic
761 dinoflagellates *Alexandrium tamarense* (= *Gonyaulax excavata*) and *A. ostenfeldii*
762 in Danish and Faroese waters. Ophelia 28, 195-213
763 Molgó, J., Aráoz, R., Benoit, E., Iorga, B.I., 2014. Cyclic imine toxins: chemistry, origin,
764 metabolism, pharmacology, toxicology, and dectection. In: Botana, L.M. (Ed.
765 Seafood and freshwater toxins (3rd edition). CRC Press, Boaca Raoton, pp 951-
766 989
767 Mouritsen, L.T., Richardson, K., 2003. Vertical microscale patchiness in nano- and
768 microplankton distributions in a stratified estuary. J. Plankton Res. 25, 783-797
769 Nagai, S., Baba, B., Miyazono, A., Tahvanainen, P., Kremp, A., Godhe, A., MacKenzie, L.,
770 Anderson, D.M., 2010. Polymorphisms of the nuclear ribosomal RNA genes found
771 in the different geographic origins in the toxic dinoflagellate *Alexandrium*
772 *ostenfeldii* and the species detection from a single cell by LAMP. DNA
773 Polymorphism 18, 122-126
774 Okolodkov, Y.B., 2005. The global distributional patterns of toxic, bloom dinoflagellates
775 recorded from the Eurasian Arctic. Hamful Algae 4, 351-369
776 Okolodkov, Y.B., Dodge, J.D., 1996. Biodiversity and biogeography of planktonic
777 dinoflagellates in the Arctic Ocean. J. Exp. Mar. Biol. Ecol. 202, 19-27
778 Paulsen, O., 1904. Plankton-investigations in the waters round Iceland in 1903. Medd.
779 Kommn. Havunders. Kobenh. Ser. Plankt. 1, 1-40
780 Posada, D., 2008. ModelTest: phylogenetic model averaging. Mol. Biol. Evol. 25, 1253-
781 1256
782 Rambaut, A., Drummond, A.J. (2007) Tracer v1.4, BEAST Software website.
783 Roach, J.S., LeBlanc, P., Lewis, N.I., Munday, R., Quilliam, M.A., MacKinnon, S.L., 2009.
784 Characterization of a Dispiroketal Spirolide Subclass from *Alexandrium*
785 *ostenfeldii*. J. Nat. Prod. 72, 1267-1240
786 Rodriguez, F., Oliver, J.L., Marin, A., Medina, J.R., 1990. The general stochastic model of
787 nucleotide substitution. J Theor. Biol. 142, 485-501
788 Ronquist, F., Huelsenbeck, J.P., 2003. MrBayes 3: Bayesian phylogenetic inderence under
789 mixed models. Bioinformatics 19, 1572-1574
790 Sánchez, S., Villanueva, P., Carbajo, L., 2004. Distribution and concentration of
791 *Alexandrium peruvianum* (Balech and de Mendiola) in the Peruvian coast
792 (03°24′–18°20′ LS) between 1982–2004. In: Abstracts, XI International
793 Conference on Harmful Algal Blooms, Cape Town, South Africa. November 15–
794 19, 2004. pp 227
795 Screen, J.A., Simmonds, I., 2012. The central role of diminishing sea ice in recent Arctic
796 temperature amplification. Nature 464, 1334-1337
797 Selina, M.S., Konovalova, G.V., Morozova, T.V., Orlova, T., 2006. Genus *Alexandrium*
798 Halim, 1960 (Dinophyta) from the Pacific Coast of Russia: Species Composition,
799 Distribution, and Dynamics. Russian Journal of Marine Biology 32, 321-332
800 Sheng, J., Malkiel, E., Katz, J., Adolf, J., Place, A.R., 2010. A dinoflagellate exploits toxins to
801 immobilize prey prior to ingestion. Proceedings of the National Academy of
802 Science of the United States of America 107, 2082-2087
803 Sleno, L., Chalmers, M.J., Volmer, D.A., 2004. Structural Study of Spirolide Marine Toxins
804 by Mass Spectrometry. Part II: Mass Spectrometric Characterization of Unknown

805 Spirolides and Related Comounds in a Cultured Phytoplankton Extract.
806 Analytical and Bioanalytical Chemistry 378, 977-986
807 Sopanen, S., Setälä, O.,¨Piiparinen, J., Erler, K., Kremp, A., 2011. The toxic dinoflagellate
808 *Alexandrium ostenfeldii* promotes incapacitation of the calanoid copepods
809 *Eurytemora affinis* and *Acartia bifilosa* from the northern Baltic Sea. J. Plankton
810 Res. 33, 1564-1573
811 Stoecker, D.K., Tillmann, U., Granéli, E., 2006. Phagotrophy in Harmful Algae. In: Granéli,
812 E., Turner, J.T. Eds. Ecology of Harmful Algae. Springer, Berlin, pp 177-187
813 Suikkanen, S., Kremp, A., Hautala, H., Krock, B., 2013. Paralytic shellfish toxins or
814 spirolides? The role of environmental and genetic factors in toxin production of
815 the *Alexandrium ostenfeldii* complex. Harmful Algae 26, 52-59
816 Tangen, K., 1983. Shellfish poisoning and the occurence of potentially toxic
817 dinoflagellates in Norwegian waters. Sarsia 68, 1-7
818 Tatters, A.O., Van Wagoner, R.M., Wright, J.L.C., Tomas, C.R., 2012. Regulation of
819 spiroimine neurotoxins and hemolytic activity in laboratory cultures of the
820 dinoflagellate *Alexandrium peruvianum* (Balech & Mendiola) Balech & Tangen.
821 Hamful Algae 19, 160-168
822 Taylor, F.J.R., Fukuyo, Y., Larsen, J., 1995. Taxonomy of harmful dinoflagellates. In:
823 Hallegraeff, G.M., Anderson, D.M., Cembella, A.D. Eds. Manual on Harmful Marine
824 Microalgae. IOC Manuals and Guides No. 33. Intergovernmental Oceanographic
825 Commission of UNESCO, Paris, Paris, pp 33–42
826 Tillmann, U., 1998. Phagotrophy by a plastidic haptophyte, *Prymnesium patelliferum*.
827 Aquat. Microb. Ecol. 14, 155-160
828 Tillmann, U., John, U., 2002. Toxic effects of *Alexandrium* spp. on heterotrophic
829 dinoflagellates: an allelochemical defence mechanism independent of PSP toxins.
830 Mar. Ecol. Prog. Ser. 230, 47-58
831 Tillmann, U., Hansen, P.J., 2009. Allelopathic effects of *Alexandrium tamarense* on other
832 algae: evidence from mixed growth experiments. Aquat. Microb. Ecol. 57, 101-
833 112
834 Tillmann, U., John, U., Cembella, A.D., 2007. On the allelochemical potency of the marine
835 dinoflagellate *Alexandrium ostenfeldii* against heterotrophic and autotrophic
836 protists. J. Plankton Res. 29, 527-543
837 Tillmann, U., Alpermann, T., John, U., Cembella, A., 2008. Allelochemical interactions and
838 short-term effects of the dinoflagellate *Alexandrium* on selected
839 photoautotrophic and heterotrophic protists. Harmful Algae 7, 52-64
840 Tillmann, U., Alpermann, T., Purificacao, R., Krock, B., Cembella, A., 2009. Intra-
841 population clonal variability in allelochemical potency of the toxigenic
842 dinoflagellate *Alexandrium tamarense*. Harmful Algae 8, 759-769
843 Tomas, C.R., Van Wagoner, R.M., Tatters, A.O., White, K.D., Hall, S., Wright, J.L.C., 2012.
844 *Alexandrium peruvianum* (Balech and Mediola) Balech and Tangen a new toxic
845 species for coastal North Carolina. Hamful Algae 17, 54-63
846 Van Wagoner, R.M., Misner, I., Tomas, C.R., Wright, J.L.C., 2011. Occurrence of 12-
847 methylgymnodimine in a spirolide-producing dinoflagellate Alexandrium
848 peruvianum and the biogenetic implications. Tetrahedon Letters 52, 4243-4246
849 Walsh, J.J., Dieterle, D.A., Chen, F.R., Lenes, J.M., Maslowski, W., Cassano, J.J., Whitledge,
850 T.E., Stockwell, D., Flint, M., Sukhanova, I.N., Christensen, J., 2011. Trophic
851 cascades and future harmful algal blooms within ice-free Arctic Seas north of
852 Bering Strait: A simulation analysis. Prog. Oceanogr. 91, 312-343

853 Wassmann, P., Carroll, J., Bellerby, R.G.J., 2008. Carbon flux and ecosystem feedback in
854 the northern Barents Sea in an era of climate change. Deep-Sea Res. PT II 55,
855 2143–2153
856 Weissbach, A., Rudström, M., Oloffson, M., Béchemin, C., Icely, J.D., Newton, A., Tillmann,
857 U., Legrand, C., 2011. Phytoplankton allelochemical interactions change
858 microbial food web dynamics. Limnol. Oceanogr. 56, 899-909
859 Yoo, Y.D., Jeong, H.J., Kim, M.S., Kang, N.S., Song, J.Y., Shin, W., Kim, K.Y., Lee, K., 2009.
860 Feeding by phototrophic red tide dinoflagellates on the ubiquitous marine
861 diatom *Skeletonema costatum*. J. Eukaryot. Microbiol. 56, 413-420
862 Zwickl, D.J. (2006) Genetic algorithm approaches for the phylogenetic analysis of large
863 biological sequence datasets under the maximum likelihood criterion. The
864 University of Texas, Texas.
865
866

867

868 **FIGURE CAPTIONS**

869

870 **Figure 1**. Map of the southern part of Greenland with sampling stations at the western and
871 southern coasts.

872

873 **Figure 2**. Light micrographs of *A. ostenfeldii* cells from field samples collected at station 524
874 containing food vacuoles. A and B representing two different focal planes of the same cell.
875 Scale bars = 15 µm

876

877 **Figure 3**. Bayesian tree derived from a concatenated ITS2-5.8-ITS2-D1/D2 LSU alignment.
878 Node labels correspond to posterior probabilities from Bayesian interference and bootstrap
879 values from maximum likelihood, ML, analyses (ML/BI).

880

881 **Figure 4**. Cell morphology. A and B: Light micrographs of a life cell of strain P2G3 in
882 ventral view at different focus. Arrows on A point to the ends of the U-shaped nucleus,
883 arrows on B emphasize visible 1' (first apical) plate with ventral pore and s.a. (anterior
884 sulcal) plate. C-H: epifluorescence micrographs of cells of strain P1G3 stained with
885 fluorescent brightener: (C) 1' and (D) doorlatch-shaped s.a. plate (arrow), (E) cell in ventral
886 view, (F) lateral plates, (G) apical plates and apical pore (arrow), and (H) sulcal plates. s.d.a.:
887 right anterior lateral sulcal plate, s.s.a.: left anterior lateral sulcal plate, s.p.: posterior sulcal
888 plate. Scale bars: A- B = 15 µm, C,D,H = 5 µm, E = 20 µm; F, G = 10 µm.

889

890 **Figure 5**. Lytic activity of 34 *A. ostenfeldii* isolates from western and southern Greenland.
891 Stations represented by different colors: white bars = Station 506, grey bars = Station 516 and
892 black bars = Station 524.

893

894 **TABLES**

895

896 Table 1: Information on analyses performed on *Alexandrium ostenfeldii* isolates from

897 Greenland

898

Strain	Station	Morphological species confirmation	Detailed morphometric analysis	Sequences	PSP toxins	Spirolides	Lyse test
P1 D5	506	x	x	SSU, ITS, LSU	x	x	x
P1 H10	516	x	x	SSU, ITS, LSU	x	x	x
P2 E3	516	x		SSU, ITS, LSU	x	x	x
P2 E4	516	x		SSU, ITS, LSU	x	x	x
P2 F2	516	x		SSU, ITS, LSU	x	x	x
P2 F3	516	x			x	x	x
P2 F4	516	x			x	x	x
P2 F7	516	x			x	x	
P2 G2	516	x			x	x	x
P2 G9	516	x		SSU, ITS, LSU	x	x	x
P2 H4	516	x			x	x	x
P2 H8	516	x			x	x	x
P3 F1	516	x	x	SSU, ITS, LSU	x	x	x
P4 C6	516	x			x	x	x
P4 E3	516	x			x	x	x
P4 D8	516	x			x	x	
P4 F10	516	x			x	x	x
P4 G2	516	x			x	x	x
P3 A12	516	x			x	x	x
P2 H2	516	x			x	x	x
P2 G3	516	x	x	SSU, ITS, LSU	x	x	x
P3 E4	516	x		SSU, ITS, LSU	x	x	x
P4 F4	516	x			x	x	x
P1 F5	524	x	x	SSU, ITS, LSU	x	x	x
P1 F7	524	x			x	x	x
P1 F8	524	x	x	SSU, ITS, LSU	x	x	x
P1 F9	524	x		SSU, ITS, LSU	x	x	x
P1 F10	524	x			x	x	x
P1 F11	524	x			x	x	x
P1 G3	524	x	x	SSU, ITS, LSU	x	x	x
P1 G5	524	x			x	x	x
P1 G11	524	x			x	x	x
P1 G8	524	x			x	x	x
P1 F6	524	x			x	x	x
P1 F4	524	x			x	x	x
P1 G6	524	x		SSU, ITS, LSU	x	x	x

899
900

901

902

903 Table 2: Mass transitions m/z (Q1>Q3 mass) and their respective cyclic imine toxins.

904

Mass transition	toxin	Collision energy (CE) [V]
508>490	GYM-A	57
522>504	12-me GYM -A	57
640>164	undescribed	57
644>164	undescribed	57
650>164	H	57
658>164	undescribed	57
674>164	undescribed	57
678>164	13,19-didesme C	57
678>150	undescribed	57
692>164	13-desme C, G, undescribed	57
692>150	A, undescribed	57
694>164	13-desme D, undescribed, pinnatoxin G	57
694>150	B	57
696>164	undescribed	57
698>164	undescribed	57
706>164	C, 20-me G	57
708>164	D	57
710>164	undescribed	57
710>150	undescribed	57
720>164	undescribed	57
722>164	undescribed	57
766>164	pinnatoxin F	57
784>164	pinnatoxin E	57

905

Table 3: Cell dimensions and plate morphometry in representative strains from the three sampling stations.

	Cell size				**Plate morphometry**						
strain	Cell width	Cell length	Cell Ratio w/h	N	1’ % straight margin	1' % Ext.	1' area (µm2)	s.a.% Door-latch	s.a. Ratio w/h	6’’ Ratio w/h	N
Station 506											
P1 D5	27.78 (±1.92)	28.83 (±2.41)	0.97 (±0.05)	25	80	0	36.19 (±4.60)	87	1.49 (±0.20)	1.17 (±0.22)	15
Station 516											
P1 H10	43.65 (±6.38)	45.78 (±6.47)	0.95 (±0.04)	25	90	20	99.50 (±18.76)	70	1.54 (±0.28)	1.23 (±0.10)	10
P3 F1	31.45 (±2.30)	33.10 (±2.71)	0.95 (±0.03)	25	87	7	60.76 (±13.41)	100	1.70 (±0.20)	1.32 (±0.13)	15
P2 G3	30.70 (±1.85)	34.53 (±2.72)	0.89 (±0.05)	25	100	47	72.43 (±16.29)	53	1.57 (±0.30)	1.34 (±0.17)	15
Station 524											
P1 F5	31.31 (±2.59)	34.09 (±3.88)	0.92 (±0.07)	25	73	0	58.69 (±10.74)	93	1.51 (±0.20)	1.34 (±0.14)	15
P1 F8	35.73 (±3.18)	37.10 (±4.07)	0.97 (±0.13)	25	80	0	68.93 (±16.03)	93	1.56 (±0.21)	1.36 (±0.14)	15
P1 G3	30.12 (±2.99)	33.19 (±2.62)	0.91 (±0.06)	25	93	7	73.56 (±16.20)	93	1.48 (±0.16)	1.36 (±0.13)	15

Table 4. Percent distribution of spirolide analogues. Numbers in bold represent relative abundances > 1%. SPX-1 = 13-desmethyl spirolide C; C = spirolide C; 20-me G = 20-methyl spirolide G; H = spirolide H: Cp = compound

	Stat	SPX-1	C	20-meG	H	Cp 1	Cp 2	Cp 3	Cp 4	Cp 5	Cp 6	Cp 7	Cp 8
P1 D5	506	-	**77.1**	**16.8**	-	-	-	-	-	-	**3.4**	**2.7**	-
P1 H10	516	0.7	-	**84.3**	-	0.1	-	0.3	-	0.8	-	-	**13.7**
P2 E3	516	**31.2**	-	-	**41.3**	-	**27.5**	-	-	-	-	-	-
P2 E4	516	**19.2**	-	-	-	1.2	-	-	-	**70.1**	-	-	**9.4**
P2 F2	516	**5.1**	**63.6**	-	**6.7**	0.1	**4.1**	-	-	**16.6**	-	**3.8**	-
P2 F3	516	-	**82.9**	**17.1**	-	-	-	-	-	-	-	-	-
P2 F4	516	**2.7**	**57.3**	**39.7**	-	-	-	-	-	-	0.1	-	-
P2 F7	516	**1.4**	**31.1**	-	**25.1**	**1.2**	**10.0**	-	-	**29.0**	-	-	**2.3**
P2 G2	516	0.2	**40.2**	**18.4**	**7.1**	-	**11.1**	-	-	**11.6**	-	-	**11.3**
P2 G9	516	-	**100.0**	-	-	-	-	-	-	-	-	-	-
P2 H4	516	-	**95.4**	**4.6**	-	-	-	-	-	-	-	-	-
P2 H8	516	**2.4**	-	**89.0**	-	-	-	-	-	0.3	-	-	**8.2**
P3 F1	516	0.2	-	**81.7**	-	-	0.1	0.2	-	**1.0**	-	-	**16.9**
P4 C6	516	-	**50.3**	**49.7**	-	-	-	-	-	-	-	-	-
P4 E3	516	1.2	**96.3**	**2.2**	-	-	-	0.3	-	-	-	-	-
P4 D8	516	-	**31.4**	-	**14.1**	-	-	**9.0**	**36.1**	**9.4**	-	-	-
P4 F10	516	-	**68.6**	**20.0**	0.2	-	-	-	-	-	-	-	**11.3**
P4 G2	516	-	-	**100.0**	-	-	-	-	-	-	-	-	-
P3 A12	516	-	**52.2**	-	**47.8**	-	-	-	-	-	-	-	-
P2 H2	516	-	-	**92.5**	-	-	-	0.9	-	-	-	-	**6.6**
P2 G3	516	**18.1**	**1.3**	0.1	-	-	-	-	-	**72.7**	-	-	**7.8**
P3 E4	516	0.2	**99.6**	-	-	-	-	0.2	-	-	-	-	-
P4 F4	516	-	**77.4**	**19.6**	0.3	-	-	0.4	-	**2.1**	-	-	-
P1 F5	524	0.1	**79.5**	**19.8**	-	-	-	0.2	-	-	0.1	0.2	-
P1 F7	524	0.1	**78.3**	**20.9**	-	-	0.1	0.4	-	-	0.1	-	-
P1 F8	524	-	**92.1**	**6.6**	-	-	0.1	0.4	-	-	0.2	0.5	-
P1 F9	524	0.2	**64.7**	**33.2**	-	-	0.1	**1.4**	-	-	0.3	-	-
P1 F10	524	0.1	**68.4**	**30.5**	-	-	0.1	0.9	-	-	0.1	-	-
P1 F11	524	-	**87.3**	**6.4**	-	-	-	-	-	-	-	**5.4**	-
P1 G3	524	0.6	**92.3**	**6.6**	-	-	-	0.6	-	-	-	-	-
P1 G5	524	0.7	**76.1**	**21.7**	0.4	-	-	0.4	-	-	0.3	0.4	-
P1 G11	524	0.2	**84.2**	**14.2**	0.5	-	-	0.3	-	-	0.3	0.3	-
P1 G8	524	-	**88.6**	**6.5**	-	-	-	-	-	-	-	**4.9**	-
P1 F6	524	0.1	**85.1**	**13.8**	-	-	0.1	0.1	-	-	0.1	0.3	-
P1 F4	524	0.1	**77.2**	**22.3**	-	-	-	-	-	-	0.1	0.2	-
P1 G6	524	-	**70.5**	**28.0**	0.3	-	-	0.6	-	-	0.2	0.3	-

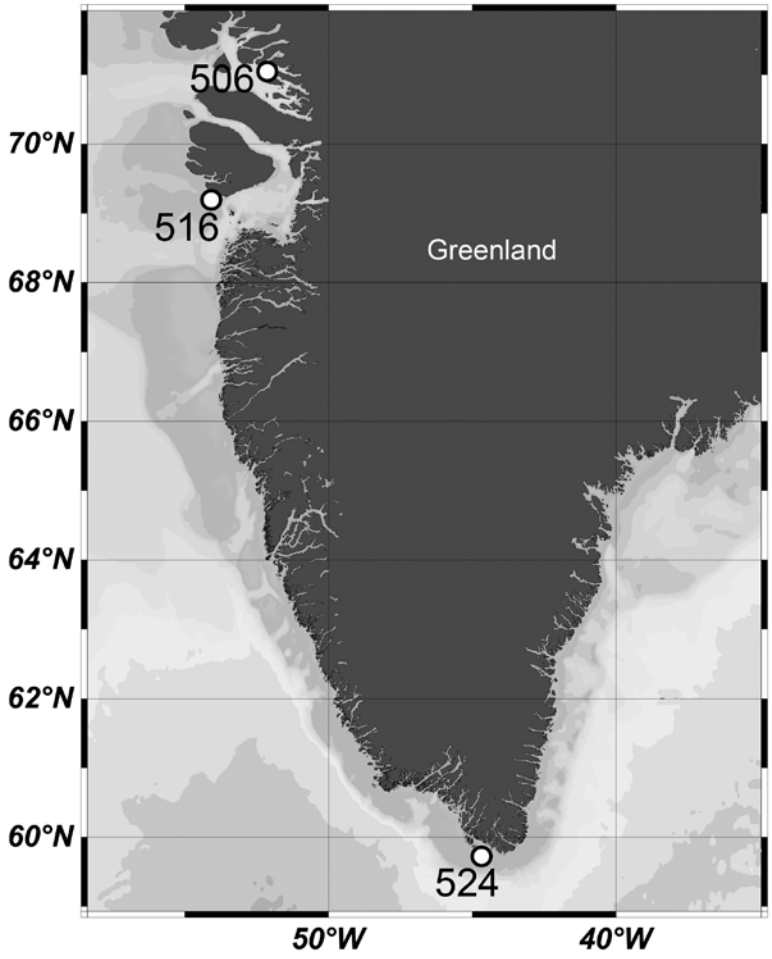

Fig. 1

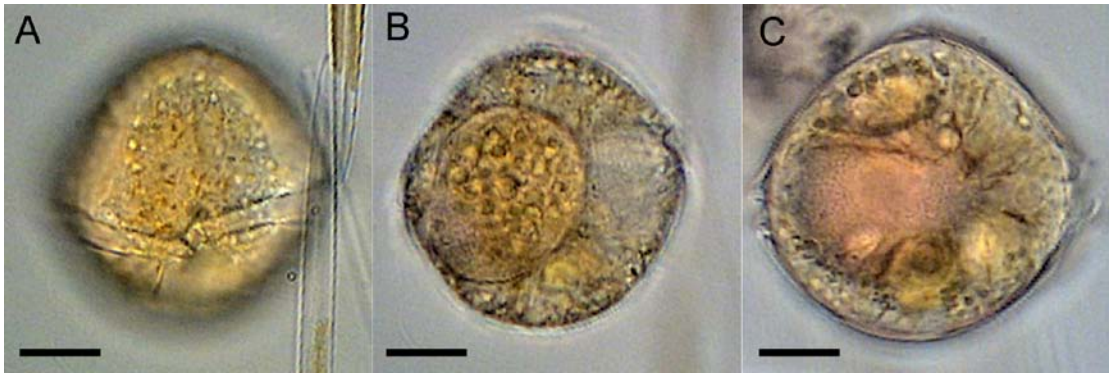

Fig. 2

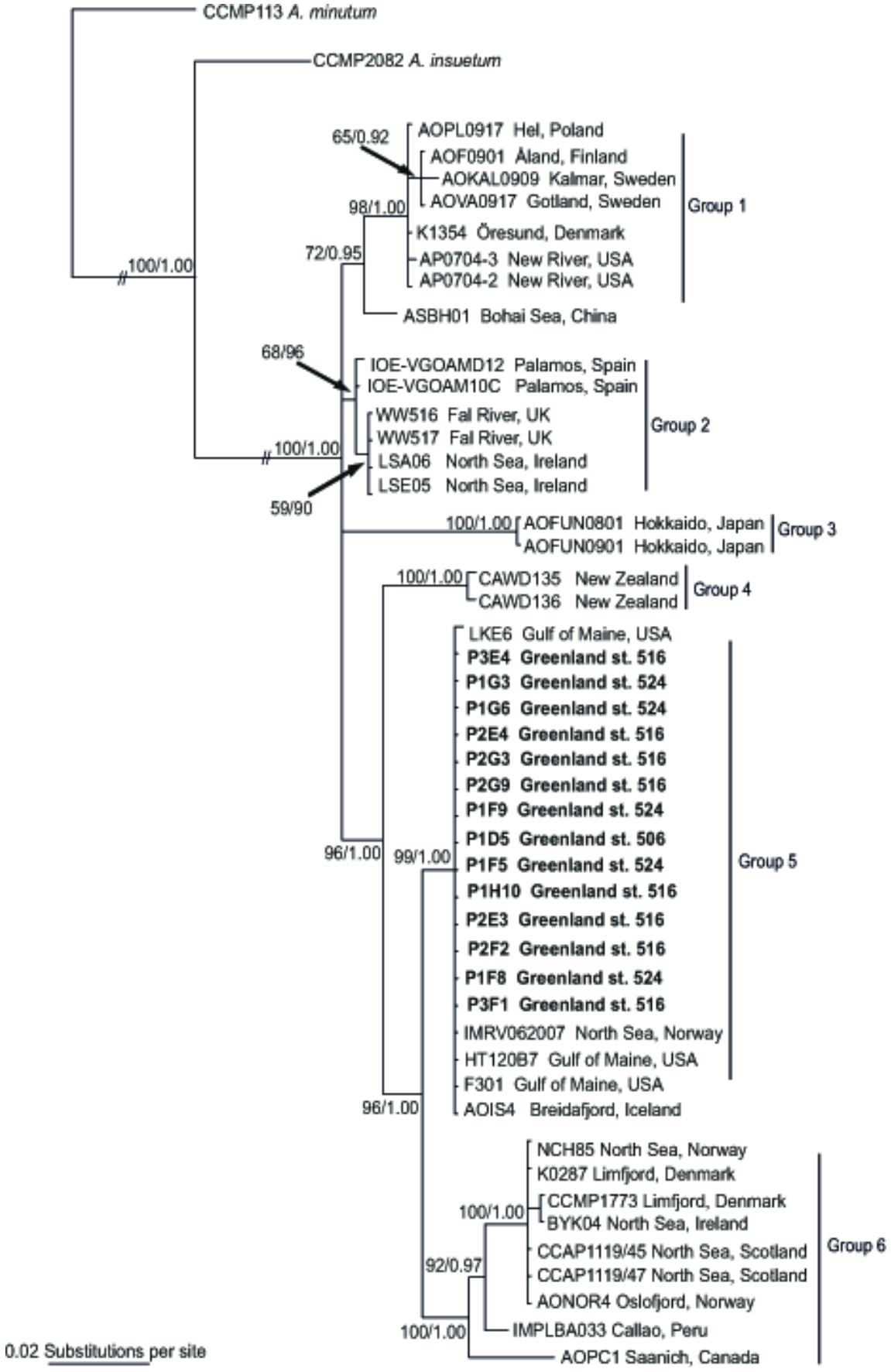
CCMP113 A. minutum
CCMP2082 A. insuetum
65/0.92
AOPL0917 Hel, Poland
AOF0901 Åland, Finland
AOKAL0909 Kalmar, Sweden
AOVA0917 Gotland, Sweden
98/1.00
K1354 Öresund, Denmark
72/0.95
AP0704-3 New River, USA
AP0704-2 New River, USA
100/1.00
ASBH01 Bohai Sea, China
Group 1
68/96
IOE-VGOAMD12 Palamos, Spain
IOE-VGOAM10C Palamos, Spain
WW516 Fal River, UK
WW517 Fal River, UK
100/1.00
LSA06 North Sea, Ireland
LSE05 North Sea, Ireland
59/90
Group 2
100/1.00
AOFUN0801 Hokkaido, Japan
AOFUN0901 Hokkaido, Japan
Group 3
100/1.00
CAWD135 New Zealand
CAWD136 New Zealand
Group 4
LKE6 Gulf of Maine, USA
P3E4 Greenland st. 516
P1G3 Greenland st. 524
P1G6 Greenland st. 524
P2E4 Greenland st. 516
P2G3 Greenland st. 516
P2G9 Greenland st. 516
P1F9 Greenland st. 524
P1D5 Greenland st. 506
96/1.00
99/1.00
P1F5 Greenland st. 524
P1H10 Greenland st. 516
P2E3 Greenland st. 516
P2F2 Greenland st. 516
P1F8 Greenland st. 524
P3F1 Greenland st. 516
IMRV062007 North Sea, Norway
HT120B7 Gulf of Maine, USA
F301 Gulf of Maine, USA
96/1.00
AOIS4 Breidafjord, Iceland
Group 5
NCH85 North Sea, Norway
K0287 Limfjord, Denmark
100/1.00
CCMP1773 Limfjord, Denmark
BYK04 North Sea, Ireland
92/0.97
CCAP1119/45 North Sea, Scotland
CCAP1119/47 North Sea, Scotland
AONOR4 Oslofjord, Norway
100/1.00
IMPLBA033 Callao, Peru
AOPC1 Saanich, Canada
Group 6
0.02 Substitutions per site

Fig. 3

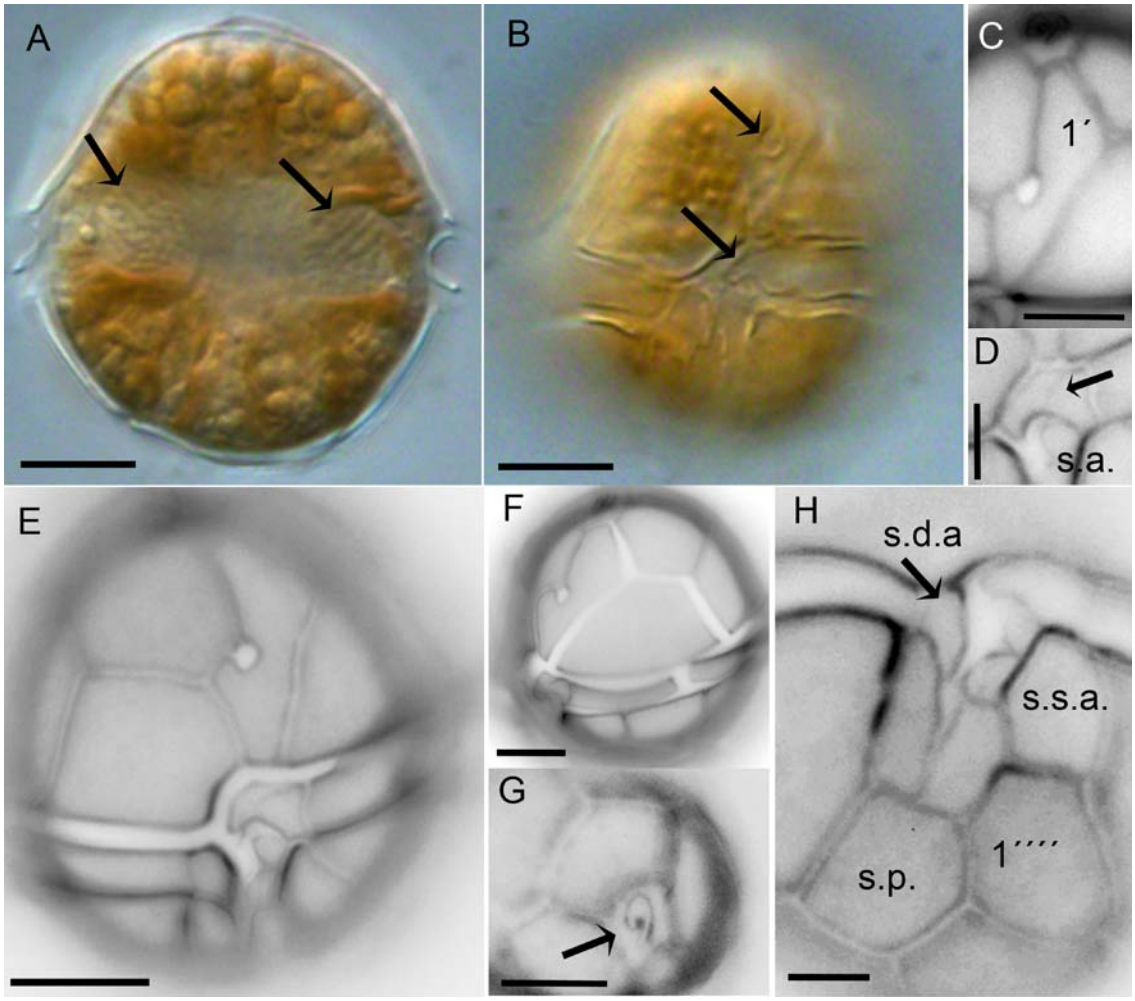

Fig. 4

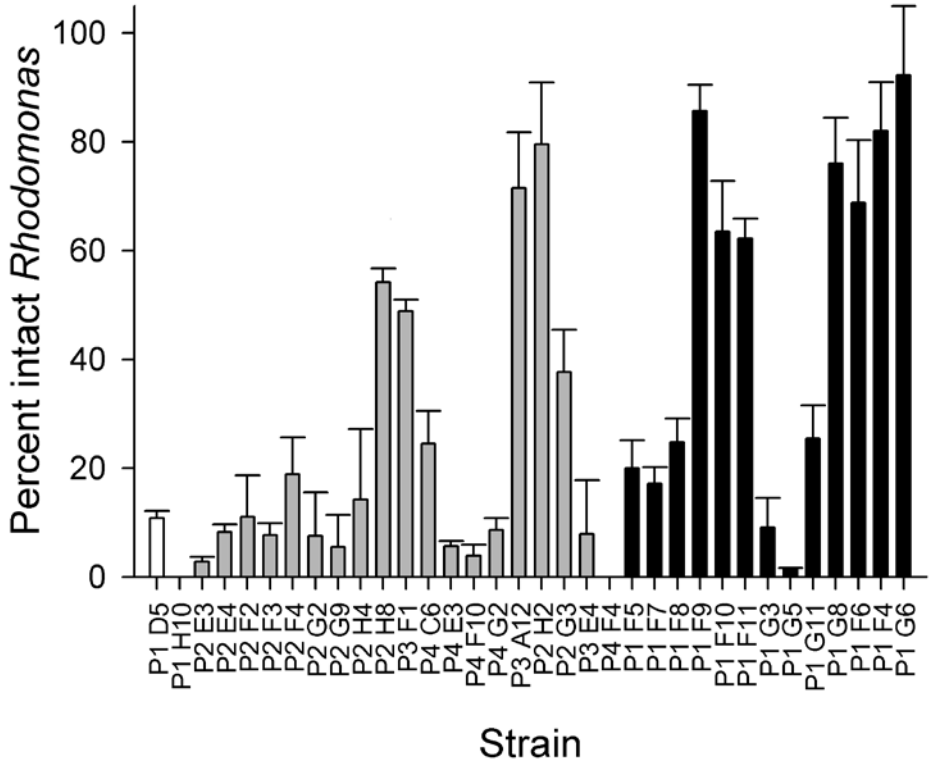
Percent intact Rhodomonas
100
80
60
40
20
0
P1 D5
P1 H10
P2 E3
P2 E4
P2 F2
P2 F3
P2 F4
P2 G2
P2 G9
P2 H4
P2 H8
P3 F1
P4 C6
P4 E3
P4 F10
P4 G2
P3 A12
P2 H2
P2 G3
P3 E4
P4 F4
P1 F5
P1 F7
P1 F8
P1 F9
P1 F10
P1 F11
P1 G3
P1 G5
P1 G11
P1 G8
P1 F6
P1 F4
P1 G6
Strain

Fig. 5